The Abdus Salam
International Centre for Theoretical Physics

United Nations
Educational, Scientific and
Cultural Organization

IAEA
International Atomic Energy Agency

2022-46

Workshop on Theoretical Ecology and Global Change

2 - 18 March 2009

Inapparent infections and cholera dynamics Supplementary Information

PASCUAL SPADA Maria Mercedes
University of Michigan
Department of Ecology and Evolutionary Biology
2019 Natural Science Bldg., 830 North University Ave.
Ann Arbor MI 48109-1048
U.S.A.

Inapparent infections and cholera dynamics
Supplementary Information

Aaron A. King[1,2], Edward L. Ionides[3], Mercedes Pascual[1,4], Menno J. Bouma[5]
Departments of [1]Ecology & Evolutionary Biology, [2]Mathematics, and [3]Statistics,
University of Michigan, Ann Arbor, MI 48109 USA
[4]Santa Fe Institute, 1399 Hyde Park Road, Santa Fe, New Mexico 87501 USA
[5]Department of Infectious and Tropical Diseases,
London School of Hygiene and Tropical Medicine,
University of London, London WC1E 7HT UK

June 4, 2008

Summary of Supplementary Information

Supplementary Equations

SIRS and two-path model equations. We let $S(t)$ denote the real-valued approximation to the (integer-valued) number of individuals in class S at time t. $I(t)$, $R_1(t)$, ..., $R_k(t)$, $Y(t)$ are defined similarly. The diagram in Fig. 1B is interpreted as a system of coupled stochastic differential equations,

$$\begin{aligned}
\frac{dS}{dt} &= k\epsilon\, R_k + \rho\, Y + \frac{dH}{dt}(t) + \delta\, H(t) - (\lambda(t) + \delta)\, S \\
\frac{dI}{dt} &= c\,\lambda(t)\, S - (m + \gamma + \delta)\, I \\
\frac{dY}{dt} &= (1-c)\,\lambda(t)\, S - (\rho + \delta)\, Y \\
\frac{dR_1}{dt} &= \gamma\, I - (k\,\epsilon + \delta)\, R_1 \\
&\vdots \\
\frac{dR_k}{dt} &= k\,\epsilon\, R_{k-1} - (k\,\epsilon + \delta)\, R_k
\end{aligned} \tag{1}$$

In the case $c = 1$, these equations collapse to the SIRS model. Environmental stochasticity enters through noise added to the time-varying force of infection, $\lambda(t)$. This is modeled by

$$\lambda(t) = \omega + [\bar{\beta}\, e^{\beta_{trend}\, t}\, \beta_{seas}(t) + \sigma\, \xi(t)]\, \frac{I(t)}{H(t)}.$$

Here $\xi(t) = dW/dt(t)$, Gaussian white noise[1]. Although the Brownian motion $W(t)$ is not differentiable, $\xi(t)$ is interpreted via the convention that $\xi(t)\, dt = dW(t)$. Multiplying Eq. 1 through by dt then gives an infinitesimal equation. The Gaussian infinitesimal $dW(t)$ is basic to the construction and solution of stochastic differential equations[2,3]. The term $\bar{\beta}\, e^{\beta_{trend}\, t}\, \beta_{seas}(t) + \sigma\, \xi(t)$ corresponds to human-to-human transmission. Seasonality of transmission is modeled by

$$\log \beta_{seas}(t) = \sum_{k=0}^{5} b_k\, s_k(t),$$

where $\{s_k(t)\}$ is a periodic cubic B-spline basis[4] defined so that $s_k(t)$ has a maximum at $t = (2k+1)/12$ and normalized so that $\sum_{k=0}^{5} s_k(t) = 1$. Here, time is measured in units of years; β_{trend} captures a long-term change in transmission rates; σ is an environmental stochasticity parameter, resulting in infinitesimal variance proportional to S^2; and ω corresponds to a non-human reservoir of disease. The scaling constant $\bar{\beta} = 1$ yr^{-1}.

All other transitions in Eq. 1 except those from S to I and Y, are modeled deterministically, ignoring demographic stochasticity. The parameter c is the probability that an exposure leads to a contagious infection; γ is the rate at which individuals recover; $1/\varepsilon$ is the mean duration of immunity; $1/\sqrt{k}$ is the coefficient of variation of the immune period; $1/\rho$ is the mean duration of short-term immunity; $1/\delta$ is the life expectancy excluding cholera mortality. Analysis of a subset of districts showed that the shape parameter $k = 3$ gave the best results. We fixed k at this value for all subsequent analyses.

The population size $H(t)$, and hence also dH/dt, are treated as known via interpolation from decadal census data. The equation for dS/dt in Eq. 1 is based on cholera mortality being a

negligible proportion of total mortality. The number of fatal cholera cases for the n-th month, $n = 1, \ldots, 600$, is modeled as $M_n = \int_{(n-1)/12}^{n/12} mI(t)\,dt$. The relationship of M_n to the observed mortality y_n is modeled by a conditional Gaussian distribution, $y_n \sim \text{normal}(M_n, \tau^2 M_n^2)$. This allows for variability in the accuracy of reporting, with variance is proportional to M_n^2. It allows for over-reporting, *e.g.,* due to misdiagnosis, as well as under-reporting.

There is some subtlety in the correct interpretation of β and ω. In the context of the models, these quantities are just two components of the force of infection: β scales that component proportional to the size of the infective pool; ω quantifies the component independent of the infective pool. From the perspective of the disease dynamics, the distinguishing property of "human-to-human" transmission is not whether it occurs through water, food, fomites, or still another route, but whether its rate is influenced by previous levels of infection in the population, *i.e.,* through a dynamical feedback. Transmission from a reservoir is from this perspective unambiguously distinguished from "human-to-human" transmission by its being effectively decoupled from the previous dynamics of the disease. This distinction is of fundamental importance for the dynamics[5,6].

Seasonality in the environmental reservoir. The models above assume that the environmental reservoir is constant in time. We can relax this assumption by letting $\omega = \omega(t)$, as we have done with the transmission rate, $\beta_{seas}(t)$. This has the effect of introducing more parameters and making the model more flexible. Because it allows for the seasonality to be explained—in whole or in part—by the environmental reservoir, it also has the potential to change the results derived using the simpler models. To model $\omega(t)$, we use the same six-knot periodic B-spline basis as before:

$$\log \frac{\omega(t)}{\bar{\omega}} = \sum_{k=0}^{5} \omega_k\, s_k(t),$$

The scaling constant $\bar{\omega} = 1\ \text{yr}^{-1}$. (Of course, the parameters ω_k are estimated entirely independently of b_k.) Maximum likelihood estimates of all parameters for this seasonal-reservoir model are presented in Table S-5. In some districts, as judged by AIC_c, there is sufficient information in the data to support the additional parameters. In all districts, however, the seasonal signal in β remains strong. Critically, the predictions of high prevalence of inapparent infection, rapidly-waning immunity, and low R_0 are robust to the inclusion of seasonality in the reservoir: estimated case fatality 0.004 ± 0.002; estimated duration of immunity, 9.6 ± 8.2 wk; estimated R_0, 1.5 ± 0.2. Moreover, as do the simpler models, this model predicts a small force of infection from the reservoir relative to the total: $1.3 \pm 0.5\%$ (mean $\pm$ SE) of all cases derive from this source of infection under the seasonal-reservoir model vs. $1.0 \pm 0.4\%$ for the SIRS model and $0.19 \pm 0.06\%$ for the two-path model.

Environmental-phage model equations. In a theoretical investigation, Jensen *et al.*[7] examined the hypothesis that build-up of ambient phage can interrupt transmission. We formulated a model to evaluate this hypothesis against the historical cholera mortality data. The environmental-phage model is built to extend the SIRS model. The equations are those of Eq. 1 with $c = 1$ with

one additional state variable:

$$\begin{aligned}
\frac{dS}{dt} &= k\epsilon\, R_k + \frac{dH}{dt}(t) + \delta\, H(t) - (\lambda_\phi(t) + \delta)\, S \\
\frac{dI}{dt} &= \lambda_\phi(t)\, S - (m + \gamma + \delta)\, I \\
\frac{dR_1}{dt} &= \gamma\, I - (k\,\epsilon + \delta)\, R_1 \\
&\vdots \\
\frac{dR_k}{dt} &= k\,\epsilon\, R_{k-1} - (k\,\epsilon + \delta)\, R_k \\
\frac{d\Phi}{dt} &= I - \mu\,\Phi
\end{aligned}$$

Here, Φ represents the effect of lytic vibriophage in the environment. Ambient phage are assumed to have first-order kinetics, with a source term proportional to the number of infections and an exponential decay term. The effect of buildup of ambient phage is to reduce the force of infection, λ_ϕ:

$$\lambda_\phi(t) = \frac{\lambda(t)}{1 + a\,\Phi(t)}$$

There are two additional parameters and one initial condition to be estimated from the data: the phage decay constant is μ, the parameter a measures the strength of the environmental phage effect.

Supplementary Methods

Algorithm: maximum likelihood via iterated filtering

Model input:

process model $f(\cdot)$, measurement model $g(\cdot|\cdot)$, data $y_1, \ldots, y_N$, times $t_0, \ldots, t_N$

Algorithmic parameters:

number of particles J, fixed lag L, number of iterations M;
cooling factor $0 < a < 1$, $b > 0$; initial state vector $X_I^{(1)}$, initial parameter vector $\theta^{(1)}$;
variance-covariance matrices Σ_I, Σ_θ.

Procedure:

1. for $m = 1$ to M
2. draw $X_I(t_0, j) \sim \text{normal}(X_I^{(m)}, a^{m-1}\Sigma_I), \quad j = 1, \ldots, J$
3. set $X_F(t_0, j) = X_I(t_0, j)$
4. draw $\theta(t_0, j) \sim \text{normal}(\theta^{(m)}, ba^{m-1}\Sigma_\theta)$
5. set $\bar{\theta}(t_0) = \theta^{(m)}$
6. for $n = 1$ to N
7. set $X_P(t_n, j) = f(X_F(t_{n-1}, j), t_{n-1}, t_n, \theta(t_{n-1}, j), W)$
8. set $w(n, j) = g(y_n | X_P(t_n, j), t_n, \theta(t_{n-1}, j))$
9. draw $k_1, \ldots, k_J$ such that $\text{Prob}[k_j = i] = w(n, i)/\sum_l w(n, l)$
10. set $X_F(t_n, j) = X_P(t_n, k_j)$
11. set $X_I(t_n, j) = X_I(t_{n-1}, k_j)$
12. draw $\theta(t_n, j) \sim \text{normal}(\theta(t_{n-1}, k_j), a^{m-1}(t_n - t_{n-1})\Sigma_\theta)$
13. set $\bar{\theta}_i(t_n)$ to be the sample mean of $\{\theta_i(t_{n-1}, k_j), j = 1, \ldots, J\}$
14. set $V_i(t_n)$ to be the sample variance of $\{\theta_i(t_n, j), j = 1, \ldots, J\}$
15. end for
16. $\theta_i^{(m+1)} = \theta_i^{(m)} + V_i(t_1) \sum_{n=1}^{N} V_i^{-1}(t_n)(\bar{\theta}_i(t_n) - \bar{\theta}_i(t_{n-1}))$
17. set $X_I^{(m+1)}$ to be the sample mean of $\{X_I(t_L, j), j = 1, \ldots, J\}$
18. end for

Return:

maximum likelihood estimate for parameters, $\hat{\theta} = \theta^{(M+1)}$;
maximum likelihood estimate for initial values, $\hat{X}(t_0) = X_I^{(M+1)}$;
maximized log likelihood estimate, $\log \mathcal{L}(\hat{\theta}) = \sum_n \log(\sum_j w(n, j)/J)$

Note:

Here, $\text{normal}(\mu, \Sigma)$ denotes a multivariate normal random variable with mean vector μ and covariance matrix Σ. $X(t_n)$ takes values in $\mathbb{R}^{d_x}$, y_n takes values in $\mathbb{R}^{d_y}$, θ takes values in $\mathbb{R}^{d_\theta}$ and has components $\{\theta_i, i = 1, \ldots, d_\theta\}$. The computationally challenging steps (6–15) correspond to a standard implementation of particle filtering[8]; many refinements are possible within the context of this algorithm. The update equation (16) is the main innovation of Ionides *et al.*[9].

Supplementary Discussion

Biological basis for short-term immunity. Our results imply that, in the vast bulk of cases, exposure to the pathogen induces a rapidly-waning protection from reinfection; they also give some clues as to the likely nature of this protection. Such protection may derive entirely from the host immune system. It is known that protection is due to the secretory IgA antibody response localized to the mucosae of the gut[10–20]. Both laboratory and field studies suggest that, following recovery, mucosal IgA levels wane on a timescale commensurate with our predictions[18,21,22]. On the other hand, it may also be that the high asymptomatic ratio and short-term protection effects derive in part from a high prevalence of coinfection with lytic bacteriophage (a mechanism distinct from the putative environmental effect of phage discussed in the preceding paragraph). Many observations have been made of such coinfection and of its protective effects[23–25], but it remains unclear how commonly phage coinfection is responsible for reducing disease severity in the field. In short, while plausible biological mechanisms for the effects revealed here exist, further work is needed to fully elucidate the immunological and ecological consequences of asymptomatic cholera infections.

Public health implications. Many decades of effort have gone into cholera vaccine research. Though reasonably effective vaccines have been developed, the protection they afford typically wanes within a short time[26]. Our results not only confirm the suspicion that this may be the best that can be hoped for, but suggest that "natural vaccination" is the key to understanding why cholera outbreaks were historically not more deadly than they were. They suggest too that even the incomplete and rapidly-waning immunity provided by an inexpensive vaccine could be effective at controlling outbreaks if applied immediately prior to an outbreak's (predicted) initiation.

Further public health implications of our findings center on what determines whether an exposure results in contagious infection and/or acquired immunity. Dose-size almost certainly plays a key role[27–31]; transmission route may as well[28,29]. Thus while a relatively small dose of live bacteria induces a severe case of cholera when the innoculum is buffered, as by food, a large dose is needed when delivery is via contaminated water[27,29,32]. Moreover, the fact that recently-shed vibrio[33] are hyperinfectious implies that within-household transmission is more likely to result in severe infection. These facts, together with the relatively small estimated magnitude of the environmental reservoir effect, suggests the need for experimental quantification of routes of transmission other than the water-borne.

Comparison with earlier models. The continuous-time mechanistic models presented here represent a distinct improvement in explanatory power over the discrete-time models that have been applied before to cholera[34,35] and other infectious diseases[36,37]. This is in part due to the greater flexibility of the continuous-time models (see Fig. S-3), which can readily include terms for environmental force of infection, seasonality in one or more transmission rates, etc. Such models can be fitted because our inference method is simulation based. The models used here, moreover, take account of measurement error in addition to process noise. Previous approaches[34,35] assumed that all variability in the data was due to process noise. Finally, time discretization itself can introduce instability into model dynamics[38]. The appearance of non-mass-action transmission terms in TSIR-type models may be attributable, at least in part, to the need to tame this instability. This departure between the discrete-time model and the continuous-time process it is meant to represent may introduce bias into the estimates obtained using discrete-time models.

Supplementary Figures

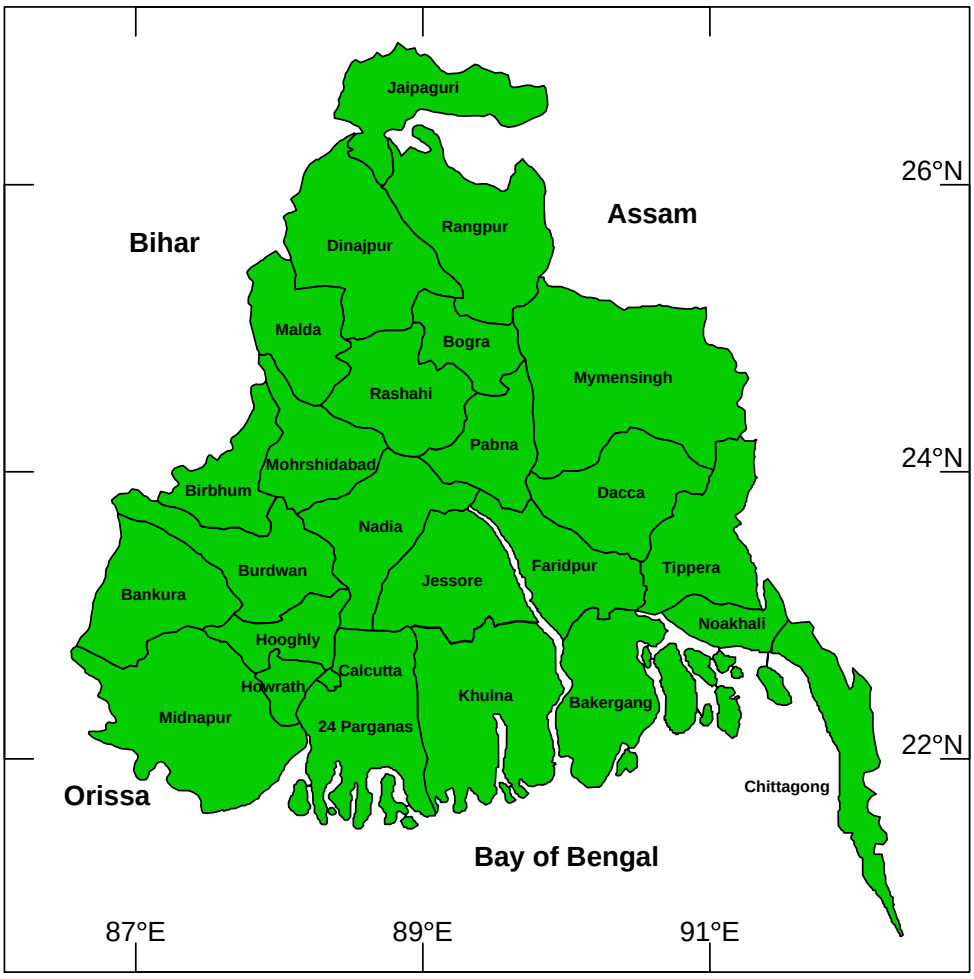

Figure S-1: **The 26 districts for which we fit models to cholera mortality data.** Data from the northern highlands district of Darjeeling were also available, but we were not successful in fitting the models to these data. This failure is likely due to the fact that, in Darjeeling district, cholera incidence is generally quite low and, in fact, the disease is entirely absent for months at a time. Our models are designed for endemic cholera dynamics and thus fail to accommodate the extremely epidemic dynamics of Darjeeling.

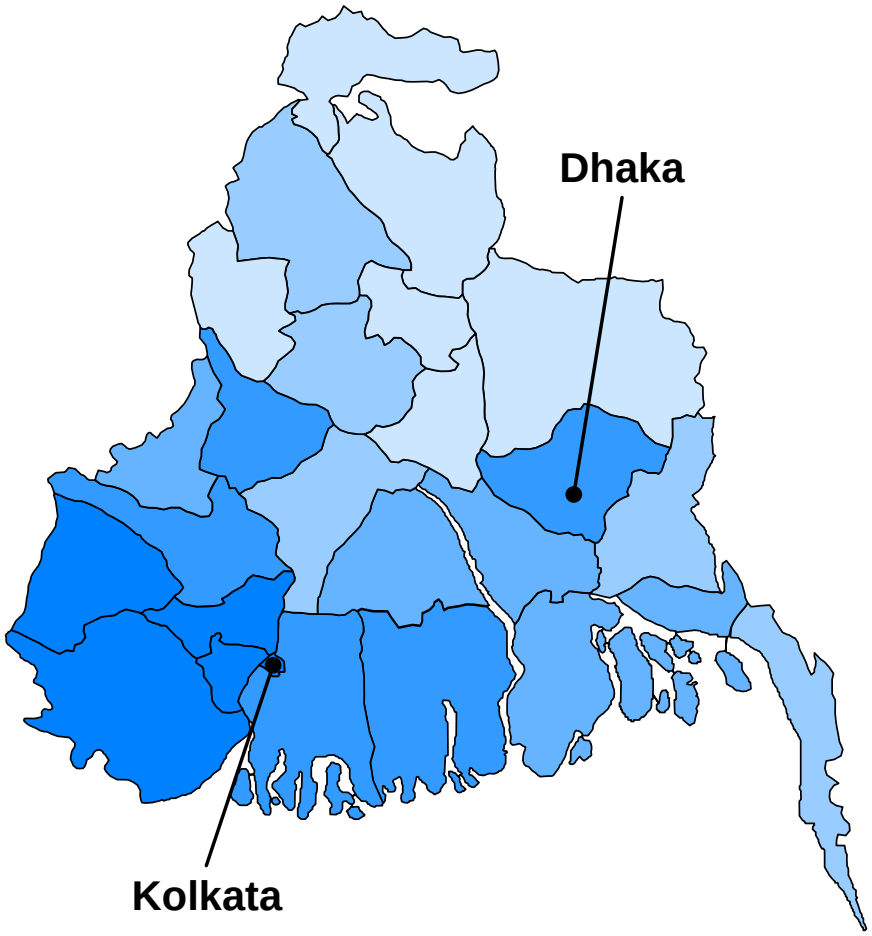

Figure S-2: **Estimates of the environmental reservoir parameter, ω, for each of the 26 districts, under the SIRS model.** Darker color corresponds to higher values of the parameter. The geographical pattern mirrors the suggestion that the southern regions of Bangladesh are the native habitat of classical cholera[39]. The pattern is similar under the two-path model. Numerical values of estimates of this and the other model parameters are provided in the Supplementary Tables.

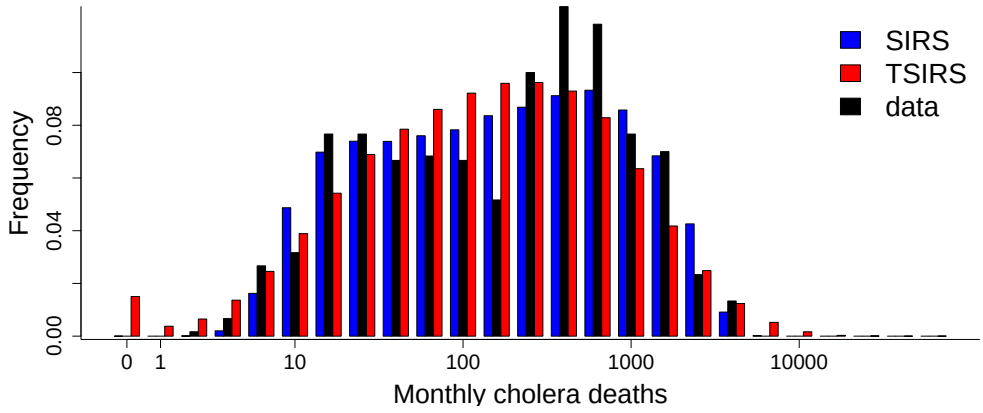

Figure S-3: **Comparison of discrete- and continuous-time model predictions.** Distributions of actual monthly deaths from the Dacca district (1891–1940, black) and simulated monthly cholera deaths from the continuous-time SIRS model with seasonal reservoir (blue) and the discrete-time TSIRS model of Koelle & Pascual[34] (red). The TSIRS model overpredicts both large epidemics and fadeouts. With fewer parameters, the continuous-time SIRS model is nevertheless considerably more flexible: the distribution it predicts is more compact and it captures some of the bimodality apparent in the data. Model parameters used correspond to the Dacca district; for each model, 200 simulated time series were used.

Supplementary Tables

Table S-1: **Model comparison for the data from Dacca**, (nowadays spelled Dhaka) the only district for which comparable analyses have been performed[34,40]. We compared models using log likelihood and second-order Akaike information criterion (AIC_c). AIC_c is defined as $-2\log\mathcal{L} + 2k + 2(k+1)/(n-k-1)$, where $\mathcal{L}$ is the likelihood, k is the number of fitted parameters and n is the number of observations. Two non-mechanistic models are used to establish a baseline for comparison. The first (seasonal mean) simply uses the monthly mean and variance in mortality. The second is a seasonal autoregressive moving-average (SARMA) model. While these models give some indication as to how predictable the data series are, they are not easy to interpret since they lack all description of mechanism. The semi-parametric method of Koelle & Pascual[34] does not lend itself to easy determination of the effective number of parameters; we report a lower bound on the AIC_c for this model. When the SIRS model is constrained to a 4 yr mean immunity, comparable to the estimate of Koelle & Pascual[34], the log likelihood (−3843.3) is also comparable. The increase in log likelihood obtained from removing the constraint $1/\varepsilon = 4$ yr is highly statistically signficant ($p < 0.001$, likelihood ratio test, $df = 1$); likewise the two-path model affords a significantly better fit ($p < 0.001$, likelihood ratio test, $df = 3$, see Supplementary Methods) than the SIRS model. Parameter estimates for all districts are in Tables S-3 through S-6.

model	log likelihood	AIC_c
SIRS with seasonal reservoir	−3763.8	7573.4
two-path	−3784.7	7610.8
environmental-phage	−3787.9	7617.2
SIRS	−3793.4	7621.9
SARMA((2,2)×(1,1))	−3804.5	7625.2
Koelle & Pascual[34]	−3840.1	> 7680.1
seasonal mean	−3989.1	8028.2

Table S-2: **Model comparison for all districts.** The quantities shown are $\Delta\mathrm{AIC}_c$, i.e., the difference in AIC_c between a given model and the best model (smallest AIC_c) for that district (denoted by $*$).

	SIRS	two-path	seasonal-reservoir	environmental-phage
Bakergang	7.4	$*$	15.4	16.5
Bankura	$*$	2.0	11.5	8.8
Birbhum	1.2	16.4	$*$	8.4
Bogra	17.0	$*$	24.7	40.9
Burdwan	50.6	63.3	$*$	56.1
Calcutta	6.2	$*$	8.9	13.9
Chittagong	19.7	13.1	23.7	$*$
Dacca	48.4	37.4	$*$	43.8
Dinajpur	5.7	11.4	17.7	$*$
Faridpur	49.8	52.6	$*$	55.5
Hooghly	40.6	53.7	$*$	47.5
Howrath	9.8	3.0	$*$	17.2
Jaipaguri	7.1	7.3	$*$	7.0
Jessore	18.2	25.4	$*$	24.9
Khulna	9.6	11.4	$*$	5.8
Malda	14.5	14.9	30.5	$*$
Midnapur	$*$	1.7	4.6	9.4
Mohrshidabad	$*$	14.1	2.1	6.5
Mymensingh	22.7	8.8	37.7	$*$
Nadia	4.1	10.4	$*$	10.1
Noakhali	4.1	$*$	5.0	11.0
Pabna	2.5	$*$	12.4	10.5
Rangpur	3.3	$*$	7.8	6.7
Rashahi	16.2	32.5	$*$	24.1
Tippera	29.9	34.0	41.3	$*$
24 Parganas	39.2	51.0	$*$	46.4

Table S-3: **Maximum likelihood estimates for the SIRS model.** The units of γ, m, ε, ω, and β_{trend} are yr^{-1}; the other quantities are dimensionless.

	$\log \mathcal{L}$	AIC_c	r^2	R_0	γ	m	ε	$\log \omega$
Bakergang	−3663.2	7361.4	0.855	1.35	11.2	0.028	36.8	−5.0
Bankura	−3039.0	6113.0	0.568	1.45	7.3	0.019	3.8	−3.5
Birbhum	−3082.4	6199.9	0.492	1.52	9.0	0.066	13.4	−4.9
Bogra	−2849.2	5733.4	0.545	1.97	14.1	0.044	2.3	−10.2
Burdwan	−3412.4	6859.9	0.584	1.48	5.0	0.043	6.2	−4.0
Calcutta	−3041.7	6118.5	0.759	1.22	16.0	0.028	51.6	−3.5
Chittagong	−3255.0	6545.1	0.709	1.53	4.9	0.043	4.1	−5.9
Dacca	−3793.4	7621.9	0.849	1.28	17.3	0.057	9.8	−4.8
Dinajpur	−2946.2	5927.4	0.501	1.64	12.3	0.021	3.5	−5.6
Faridpur	−3661.8	7358.7	0.785	1.31	19.3	0.066	6.2	−5.0
Hooghly	−3248.6	6532.2	0.575	1.09	7.1	0.019	10.1	−2.3
Howrath	−3372.1	6779.2	0.769	1.33	7.7	0.041	6.4	−3.7
Jaipaguri	−2391.1	4817.3	0.592	1.41	22.9	0.104	3.4	−9.4
Jessore	−3500.9	7036.9	0.750	1.57	15.8	0.036	12.0	−5.2
Khulna	−3508.8	7052.7	0.722	1.40	8.0	0.024	32.3	−4.3
Malda	−2903.4	5841.8	0.589	1.73	25.5	0.090	3.1	−10.9
Midnapur	−3881.5	7798.1	0.670	1.32	5.4	0.014	21.7	−2.3
Mohrshidabad	−3400.7	6836.5	0.624	1.69	11.3	0.036	5.9	−4.8
Mymensingh	−3989.7	8014.4	0.803	1.36	17.3	0.069	9.2	−8.3
Nadia	−3403.3	6841.6	0.732	1.63	12.2	0.032	27.4	−5.4
Noakhali	−3477.0	6989.0	0.695	1.80	6.0	0.032	2.6	−5.0
Pabna	−3288.3	6611.6	0.694	1.48	23.0	0.102	3.7	−9.5
Rangpur	−3269.0	6573.1	0.633	1.52	14.7	0.070	1.9	−7.4
Rashahi	−3301.9	6638.8	0.694	1.48	16.6	0.056	5.3	−5.8
Tippera	−3647.8	7330.6	0.763	1.50	11.4	0.017	23.9	−5.4
24 Parganas	−3777.8	7590.7	0.844	1.35	6.3	0.034	15.4	−3.8

	$\beta_{trend} \times 10^3$	b_0	b_1	b_2	b_3	b_4	b_5	σ	τ
Bakergang	−5.1	0.1	7.1	−8.6	1.9	2.1	5.3	2.6	0.33
Bankura	−3.2	3.0	3.1	0.7	4.9	−2.6	2.6	3.7	0.48
Birbhum	−5.1	1.7	3.8	0.6	4.4	0.4	4.4	4.0	0.53
Bogra	−6.6	2.3	4.7	1.9	3.4	3.9	3.3	4.9	0.66
Burdwan	−8.8	1.7	4.7	−6.0	1.6	1.6	3.0	3.5	0.38
Calcutta	−4.7	3.0	3.8	2.1	2.2	3.3	3.1	2.1	0.23
Chittagong	−10.7	−0.8	4.8	−0.5	1.0	0.7	4.6	3.0	0.42
Dacca	−5.0	1.2	6.2	−3.4	3.9	3.2	4.3	3.2	0.25
Dinajpur	−5.1	1.9	4.2	2.3	1.8	3.6	3.6	4.3	0.63
Faridpur	−3.0	1.4	6.5	−3.6	4.3	3.0	4.5	3.4	0.39
Hooghly	−9.0	0.5	5.8	−6.6	1.1	2.2	3.3	3.0	0.35
Howrath	−4.1	2.3	3.4	−0.7	1.9	2.5	3.1	2.3	0.20
Jaipaguri	−1.8	3.1	4.3	3.2	3.3	3.6	3.3	4.0	0.69
Jessore	−3.5	1.5	5.6	−1.2	3.4	3.4	4.6	4.1	0.39
Khulna	−7.0	−1.1	6.7	−6.5	1.4	2.8	4.6	2.6	0.36
Malda	−2.3	2.8	4.8	3.0	3.6	4.3	4.1	5.2	0.62
Midnapur	−10.0	2.0	2.8	−2.9	2.0	1.4	3.4	2.9	0.28
Mohrshidabad	−4.9	1.9	4.6	0.2	3.8	3.0	3.5	4.4	0.41
Mymensingh	−2.6	1.7	4.9	0.9	3.0	3.7	3.9	3.0	0.28
Nadia	−7.3	1.2	5.9	−2.5	2.0	4.2	3.7	4.1	0.47
Noakhali	−6.8	−1.4	7.0	−6.7	3.3	1.6	5.0	3.9	0.39
Pabna	−1.9	2.1	5.7	0.6	4.1	4.0	3.8	4.0	0.51
Rangpur	−6.6	1.2	5.3	0.8	3.4	3.5	3.6	4.1	0.62
Rashahi	−5.7	1.6	5.3	0.7	3.2	3.5	4.1	4.1	0.48
Tippera	−4.7	1.5	4.8	−2.5	3.3	2.8	4.4	3.1	0.40
24 Parganas	−6.0	0.8	4.5	−6.7	1.8	1.3	4.6	2.5	0.16

Table S-4: **Maximum likelihood estimates for the two-path model.** The units of γ, m, ε, ω, and β_{trend} are yr^{-1}; the other quantities are dimensionless

	$\log \mathcal{L}$	AIC_c	r^2	R_0	γ	m	ρ	ε	$\log \omega$	c
Bakergang	−3656.3	7354.0	0.857	1.38	7.1	2.740	8.5	0.5	−4.5	0.0088
Bankura	−3036.8	6115.0	0.556	1.41	11.0	2.494	4.5	0.3	−4.6	0.0107
Birbhum	−3086.8	6215.0	0.492	1.61	1.3	6.417	5.3	0.5	−4.4	0.0079
Bogra	−2837.5	5716.4	0.522	2.30	21.6	0.240	2.6	0.4	−10.9	0.2400
Burdwan	−3415.6	6872.7	0.580	1.44	1.8	4.135	4.3	1.0	−3.5	0.0079
Calcutta	−3035.4	6112.3	0.762	1.27	11.3	4.662	5.6	0.7	−4.3	0.0104
Chittagong	−3248.5	6538.5	0.713	1.43	8.4	3.627	4.7	0.6	−5.5	0.0113
Dacca	−3784.7	7610.8	0.852	1.29	8.0	9.238	7.1	0.7	−4.5	0.0051
Dinajpur	−2945.8	5933.1	0.508	1.87	4.3	1.304	3.0	0.7	−4.6	0.0057
Faridpur	−3660.0	7361.5	0.783	1.34	10.7	8.661	7.1	0.7	−5.0	0.0056
Hooghly	−3251.9	6545.3	0.573	1.11	3.2	4.406	5.1	0.8	−2.3	0.0040
Howrath	−3365.5	6772.4	0.771	1.32	11.2	5.262	5.7	0.6	−4.4	0.0114
Jaipaguri	−2388.1	4817.6	0.585	1.47	23.9	0.155	17.0	3.3	−9.8	0.4598
Jessore	−3501.3	7044.1	0.750	1.63	9.6	4.197	9.2	1.7	−4.6	0.0053
Khulna	−3506.5	7054.5	0.720	1.44	4.2	3.941	7.2	0.7	−4.2	0.0053
Malda	−2900.3	5842.1	0.592	1.63	29.3	0.134	22.9	2.8	−10.6	0.4809
Midnapur	−3879.2	7799.8	0.674	1.31	10.9	3.737	5.9	0.5	−3.7	0.0099
Mohrshidabad	−3404.6	6850.6	0.623	1.82	6.0	3.649	3.3	0.4	−4.3	0.0079
Mymensingh	−3979.5	8000.5	0.804	1.44	13.6	3.831	2.5	0.4	−7.9	0.0279
Nadia	−3403.3	6848.0	0.733	1.66	6.7	5.164	9.2	0.9	−5.3	0.0054
Noakhali	−3471.7	6984.9	0.691	1.71	9.5	3.103	4.4	0.5	−5.3	0.0108
Pabna	−3283.8	6609.0	0.695	1.47	12.3	13.756	4.4	0.8	−7.5	0.0059
Rangpur	−3264.2	6569.8	0.631	1.55	17.3	0.134	14.0	1.4	−7.8	0.3894
Rashahi	−3306.8	6655.1	0.691	1.52	9.0	4.285	5.8	0.8	−5.1	0.0079
Tippera	−3646.6	7334.7	0.763	1.53	7.5	3.267	5.2	3.2	−5.2	0.0056
24 Parganas	−3780.6	7602.6	0.844	1.38	2.8	3.889	4.7	0.8	−3.7	0.0079

	$\beta_{trend} \times 10^3$	b_0	b_1	b_2	b_3	b_4	b_5	σ	τ
Bakergang	−4.8	4.0	13.2	−10.7	2.8	6.8	10.2	308.3	0.31
Bankura	−4.5	7.9	7.7	6.9	8.4	6.1	7.6	334.8	0.47
Birbhum	−5.2	6.1	9.1	4.5	9.6	4.5	9.4	539.7	0.53
Bogra	−7.4	4.5	6.5	4.3	5.4	5.7	5.5	27.7	0.65
Burdwan	−9.7	6.3	9.7	0.1	8.1	5.6	8.5	448.6	0.39
Calcutta	−5.7	7.6	8.3	6.7	6.9	7.9	7.6	201.9	0.23
Chittagong	−6.8	6.0	8.9	6.2	7.5	6.2	8.8	288.7	0.44
Dacca	−6.8	6.5	11.4	2.1	9.0	8.6	9.5	639.6	0.23
Dinajpur	−10.5	4.2	10.7	4.2	4.4	8.9	8.7	694.1	0.63
Faridpur	−3.6	6.7	11.4	2.3	9.5	8.3	9.6	594.9	0.38
Hooghly	−9.4	6.7	10.7	1.2	6.7	7.9	8.5	757.2	0.35
Howrath	−2.5	7.6	8.0	6.7	7.4	7.6	7.9	202.3	0.20
Jaipaguri	−1.5	4.0	5.1	4.3	4.0	4.5	4.1	9.5	0.68
Jessore	−4.5	6.3	11.3	2.6	8.5	8.5	9.9	799.7	0.38
Khulna	−8.0	4.5	11.6	−0.5	6.9	8.0	9.7	491.0	0.36
Malda	−2.1	3.7	5.5	4.0	4.3	5.1	4.8	10.6	0.63
Midnapur	−5.0	7.8	7.3	7.2	7.5	7.3	8.1	275.8	0.29
Mohrshidabad	−5.9	6.3	9.9	3.8	8.8	7.7	8.5	585.2	0.42
Mymensingh	−5.8	5.4	8.5	4.6	6.6	7.4	7.4	114.2	0.28
Nadia	−7.6	6.3	11.3	2.0	7.3	9.3	8.9	773.1	0.46
Noakhali	−3.5	5.9	9.3	5.5	8.2	6.9	9.2	383.3	0.38
Pabna	−2.2	7.6	10.6	6.4	9.2	9.2	9.0	713.7	0.50
Rangpur	−5.1	2.9	5.9	2.6	4.4	4.7	4.5	11.1	0.61
Rashahi	−8.6	5.3	10.8	3.7	8.1	8.0	9.2	524.0	0.48
Tippera	−5.2	6.7	10.3	1.2	8.4	8.0	9.5	567.3	0.40
24 Parganas	−5.7	5.7	9.3	−0.5	7.0	6.2	9.5	329.5	0.16

Table S-5: **Maximum likelihood estimates for the seasonal-reservoir model.** The units of γ, m, ε, and β_{trend} are yr^{-1}; the other quantities are dimensionless.

	$\log \mathcal{L}$	AIC_c	r^2	R_0	γ	m	ε	b_0	b_1	b_2	b_3	b_4	b_5
Bakergang	−3661.8	7369.4	0.855	1.35	11.2	0.029	36.7	0.1	7.1	−8.7	1.9	2.2	5.2
Bankura	−3039.3	6124.5	0.570	1.40	7.4	0.019	3.9	3.0	3.0	0.6	4.9	−2.6	2.7
Birbhum	−3076.4	6198.6	0.499	1.50	9.0	0.068	13.2	1.6	3.7	0.6	4.3	0.5	4.4
Bogra	−2847.7	5741.1	0.540	1.90	14.1	0.042	2.1	2.2	4.7	1.6	3.5	3.9	3.3
Burdwan	−3381.8	6809.3	0.610	1.50	5.3	0.046	6.6	1.7	4.8	−6.0	1.5	1.8	3.3
Calcutta	−3037.7	6121.2	0.761	1.20	16.1	0.030	51.9	3.0	3.8	2.1	2.2	3.3	3.0
Chittagong	−3251.6	6549.0	0.713	1.52	5.3	0.046	3.7	−0.5	4.9	−0.5	0.8	1.0	4.5
Dacca	−3763.8	7573.4	0.858	1.22	18.0	0.064	10.6	1.2	6.2	−3.5	3.7	3.4	4.2
Dinajpur	−2946.8	5939.4	0.499	1.62	12.3	0.021	3.2	1.8	4.2	2.3	1.8	3.8	3.5
Faridpur	−3631.6	7309.0	0.800	1.26	20.6	0.071	6.6	1.4	6.5	−3.6	4.3	3.2	4.5
Hooghly	−3222.9	6491.6	0.604	1.05	7.6	0.022	10.0	0.4	5.8	−6.7	1.0	2.4	3.3
Howrath	−3361.8	6769.4	0.773	1.30	7.9	0.043	6.6	2.3	3.4	−0.7	2.0	2.5	3.1
Jaipaguri	−2382.3	4810.3	0.599	1.39	21.9	0.109	3.2	3.1	4.3	3.2	3.1	3.5	3.1
Jessore	−3486.5	7018.7	0.760	1.54	16.1	0.037	12.8	1.5	5.6	−1.3	3.3	3.5	4.5
Khulna	−3498.7	7043.1	0.726	1.38	8.1	0.024	33.0	−1.1	6.7	−6.8	1.4	2.9	4.5
Malda	−2906.0	5857.8	0.587	1.68	25.5	0.090	3.2	2.8	4.7	3.0	3.5	4.3	4.0
Midnapur	−3878.5	7802.7	0.675	1.31	5.4	0.014	22.1	2.0	2.7	−2.9	1.9	1.5	3.4
Mohrshidabad	−3396.4	6838.5	0.627	1.68	11.5	0.037	5.7	1.9	4.5	0.3	3.6	3.1	3.5
Mymensingh	−3991.8	8029.4	0.805	1.34	17.3	0.068	9.0	1.7	4.8	0.8	3.0	3.7	3.9
Nadia	−3395.9	6837.6	0.739	1.60	12.3	0.033	27.3	1.2	5.9	−2.6	2.0	4.2	3.6
Noakhali	−3472.1	6989.9	0.698	1.81	6.0	0.032	2.5	−1.4	6.9	−6.7	3.3	1.6	5.0
Pabna	−3287.9	6621.5	0.690	1.45	23.0	0.103	3.8	2.2	5.6	0.6	4.0	4.0	3.7
Rangpur	−3265.9	6577.6	0.633	1.63	14.6	0.065	1.5	1.4	5.2	1.1	3.4	3.7	3.5
Rashahi	−3288.4	6622.6	0.701	1.42	17.1	0.059	5.4	1.5	5.3	0.6	3.1	3.5	4.1
Tippera	−3648.1	7341.9	0.765	1.53	11.4	0.016	24.0	1.6	4.9	−2.6	3.3	2.8	4.4
24 Parganas	−3752.9	7551.5	0.853	1.29	6.8	0.037	15.5	0.8	4.5	−6.8	1.8	1.5	4.6

	$\beta_{trend} \times 10^3$	σ	τ	ω_0	ω_1	ω_2	ω_3	ω_4	ω_5
Bakergang	−4.6	2.5	0.32	−4.5	−4.9	−4.8	−4.7	−5.5	−4.4
Bankura	−5.2	3.8	0.47	−3.7	−3.2	−3.9	−3.8	−3.3	−4.0
Birbhum	−6.1	4.1	0.53	−4.4	−4.3	−4.9	−5.7	−5.8	−4.7
Bogra	−7.1	4.9	0.68	−9.7	−9.8	−10.2	−12.9	−10.2	−10.8
Burdwan	−10.2	3.6	0.35	−3.9	−3.7	−3.5	−2.5	−4.9	−5.4
Calcutta	−4.9	2.2	0.22	−3.6	−3.3	−3.1	−3.8	−4.0	−3.1
Chittagong	−11.8	3.0	0.41	−5.2	−5.0	−5.3	−5.8	−6.6	−6.1
Dacca	−4.8	3.1	0.22	−3.4	−4.0	−4.1	−4.1	−6.6	−4.7
Dinajpur	−7.2	4.4	0.69	−5.2	−6.1	−5.3	−5.9	−6.4	−5.4
Faridpur	−2.7	3.4	0.35	−4.0	−4.5	−3.7	−4.4	−7.1	−4.0
Hooghly	−9.3	3.1	0.35	−1.9	−1.8	−1.8	−1.7	−3.8	−2.6
Howrath	−4.0	2.3	0.19	−3.6	−2.6	−2.6	−3.6	−3.9	−4.4
Jaipaguri	−2.5	4.2	0.74	−8.8	−9.3	−10.1	−10.7	−11.2	−7.8
Jessore	−4.4	4.2	0.38	−4.7	−4.9	−4.0	−4.5	−6.6	−5.2
Khulna	−7.9	2.6	0.35	−3.7	−4.0	−2.9	−3.6	−5.5	−4.1
Malda	−0.8	4.9	0.65	−11.0	−10.9	−11.0	−11.0	−11.0	−11.0
Midnapur	−11.3	2.9	0.27	−1.8	−3.2	−2.2	−2.3	−3.1	−2.3
Mohrshidabad	−5.7	4.4	0.40	−4.5	−5.0	−5.0	−4.0	−5.8	−5.0
Mymensingh	−2.3	3.0	0.27	−8.3	−8.3	−8.3	−8.4	−8.3	−8.3
Nadia	−8.6	4.2	0.47	−5.1	−5.0	−4.9	−4.7	−6.8	−5.8
Noakhali	−9.7	3.9	0.39	−4.3	−4.1	−4.7	−4.9	−5.9	−4.4
Pabna	−2.6	3.9	0.52	−8.9	−9.2	−9.5	−9.8	−9.4	−9.9
Rangpur	−7.7	4.6	0.69	−6.7	−7.5	−7.0	−8.0	−8.5	−7.9
Rashahi	−6.5	4.1	0.48	−5.3	−5.4	−5.0	−5.1	−7.0	−6.6
Tippera	−5.1	3.2	0.40	−5.2	−5.4	−5.0	−5.1	−5.8	−5.1
24 Parganas	−5.1	2.5	0.15	−2.9	−3.4	−3.2	−2.6	−5.0	−4.7

Table S-6: **Maximum likelihood estimates for the environmental-phage model.** The units of γ, m, ε, ω, β_{trend}, a, and μ are yr^{-1}; the other quantities are dimensionless.

	$\log \mathcal{L}$	AIC_c	r^2	R_0	$\log a$	μ	γ	m	ε
Bakergang	−3664.5	7370.4	0.855	1.41	−17.3	0.32	11.2	0.028	39.8
Bankura	−3040.2	6121.8	0.570	1.40	−17.0	0.37	7.3	0.019	4.0
Birbhum	−3082.8	6207.0	0.495	1.53	−15.5	0.35	9.1	0.070	13.9
Bogra	−2857.9	5757.3	0.536	2.05	−13.1	3.66	14.1	0.042	1.9
Burdwan	−3412.0	6865.5	0.584	1.43	−15.5	2.21	5.1	0.045	6.4
Calcutta	−3042.3	6126.2	0.760	1.23	−16.7	0.36	16.2	0.030	52.4
Chittagong	−3241.9	6525.3	0.714	2.02	−9.5	8.81	4.9	0.046	4.1
Dacca	−3787.9	7617.2	0.851	1.28	−17.5	1.11	17.3	0.057	10.5
Dinajpur	−2940.1	5921.7	0.494	2.00	−8.8	23.94	11.7	0.024	3.7
Faridpur	−3661.5	7364.4	0.786	1.31	−16.9	0.50	19.0	0.066	5.9
Hooghly	−3248.8	6539.1	0.575	1.11	−16.5	0.10	7.1	0.021	9.1
Howrath	−3372.6	6786.6	0.769	1.36	−18.5	0.18	7.7	0.039	6.6
Jaipaguri	−2387.9	4817.3	0.588	1.66	−12.3	0.14	21.9	0.112	3.8
Jessore	−3501.1	7043.6	0.748	1.57	−17.1	1.30	15.6	0.035	12.7
Khulna	−3503.7	7048.9	0.723	1.39	−17.5	4.07	8.0	0.023	33.5
Malda	−2892.9	5827.3	0.578	1.86	−8.5	8.32	25.5	0.134	3.7
Midnapur	−3883.0	7807.5	0.671	1.34	−16.9	0.75	5.4	0.014	21.5
Mohrshidabad	−3400.7	6842.9	0.626	1.71	−16.4	0.68	11.3	0.037	5.4
Mymensingh	−3975.1	7991.7	0.812	1.64	−10.4	7.17	16.6	0.102	13.2
Nadia	−3403.1	6847.7	0.734	1.70	−14.6	1.79	12.2	0.033	27.0
Noakhali	−3477.2	6995.9	0.694	1.84	−17.2	0.47	5.9	0.031	2.6
Pabna	−3289.0	6619.5	0.690	1.48	−18.1	0.06	23.0	0.096	3.8
Rangpur	−3267.5	6576.5	0.629	1.79	−13.5	0.35	14.2	0.067	1.5
Rashahi	−3302.6	6646.7	0.694	1.47	−16.1	0.45	16.6	0.059	5.3
Tippera	−3629.6	7300.7	0.771	2.02	−11.1	6.95	11.0	0.022	26.8
24 Parganas	−3778.2	7597.9	0.844	1.38	−17.4	0.47	6.3	0.032	18.6

	$\log \omega$	$\beta_{trend} \times 10^3$	b_0	b_1	b_2	b_3	b_4	b_5	σ	τ
Bakergang	−4.9	−3.5	0.1	7.2	−9.0	2.2	2.1	5.3	2.6	0.32
Bankura	−3.5	−5.9	3.0	3.1	0.6	4.9	−2.6	2.6	3.9	0.48
Birbhum	−5.0	−4.8	1.8	3.7	0.7	4.3	0.4	4.4	4.1	0.53
Bogra	−11.0	−8.0	2.3	4.9	1.7	3.5	4.0	3.4	5.4	0.67
Burdwan	−3.9	−9.5	1.6	4.8	−6.0	1.3	1.5	3.1	3.4	0.38
Calcutta	−3.4	−7.0	3.1	3.8	2.2	2.2	3.3	3.1	2.3	0.22
Chittagong	−5.7	−9.2	−0.6	5.4	−0.6	1.4	0.9	4.8	4.1	0.40
Dacca	−4.6	−7.3	1.3	6.1	−3.3	3.7	3.3	4.3	3.3	0.23
Dinajpur	−5.7	−6.9	2.0	4.4	2.5	1.7	3.8	3.8	5.4	0.68
Faridpur	−4.9	−3.4	1.4	6.4	−3.6	4.3	3.0	4.4	3.4	0.38
Hooghly	−2.2	−7.7	0.6	5.9	−6.8	0.8	2.2	3.3	3.2	0.35
Howrath	−3.6	−4.0	2.3	3.4	−0.4	1.9	2.4	3.1	2.4	0.20
Jaipaguri	−9.8	−2.3	3.3	4.5	3.4	3.3	3.6	3.4	5.0	0.74
Jessore	−5.2	−4.3	1.5	5.6	−1.2	3.3	3.4	4.5	4.1	0.39
Khulna	−4.2	−8.5	−1.1	6.8	−6.9	1.4	2.8	4.5	2.5	0.35
Malda	−10.9	−1.7	2.8	4.8	3.1	3.7	4.3	4.3	5.6	0.65
Midnapur	−2.2	−11.1	2.2	2.6	−2.8	1.9	1.4	3.4	3.1	0.28
Mohrshidabad	−4.8	−5.4	2.0	4.5	0.3	3.7	3.1	3.5	4.5	0.40
Mymensingh	−8.3	−4.4	2.0	5.0	1.1	3.1	3.8	4.1	3.7	0.25
Nadia	−5.5	−8.4	1.2	6.0	−2.6	2.3	4.1	3.7	4.4	0.47
Noakhali	−5.0	−8.3	−1.3	7.0	−6.8	3.3	1.6	5.1	3.9	0.39
Pabna	−9.5	−2.9	2.1	5.7	0.5	4.1	4.0	3.8	4.0	0.52
Rangpur	−7.4	−7.5	1.5	5.3	1.1	3.4	3.8	3.6	4.9	0.69
Rashahi	−5.8	−6.2	1.6	5.2	0.6	3.2	3.5	4.1	4.1	0.48
Tippera	−5.3	−1.5	2.0	5.3	−2.4	3.5	3.0	4.5	4.5	0.37
24 Parganas	−3.8	−5.0	0.8	4.6	−7.1	1.8	1.3	4.6	2.5	0.16

Supplementary References

1. Karlin, S. & Taylor, H. M. *A Second Course in Stochastic Processes* (Academic Press, New York, 1981).

2. Øksendal, B. *Stochastic Differential Equations* (Springer, New York, 1998), 5th edn.

3. Kloeden, P. E. & Platen, E. *Numerical Soluion of Stochastic Differential Equations* (Springer, New York, 1999), 3rd edn.

4. Powell, M. J. D. *Approximation Theory and Methods* (Cambridge University Press, Cambridge, 1981).

5. Hartley, D. M., Morris, J. G. & Smith, D. L. Hyperinfectivity: a critical element in the ability of *V. cholerae* to cause epidemics? *PLoS Medicine* **3**, 63–69 (2006).

6. Pascual, M., Koelle, K. & Dobson, A. P. Hyperinfectivity in cholera: a new mechanism for an old epidemiological model? *PLoS Medicine* **3**, e280 (2006).

7. Jensen, M. A., Faruque, S. M., Mekalanos, J. J. & Levin, B. R. Modeling the role of bacteriophage in the control of cholera outbreaks. *Proceedings of the National Academy of Sciences of the U.S.A.* **103**, 4652–4657 (2006).

8. Arulampalam, M. S., Maskell, S., Gordon, N. & Clapp, T. A tutorial on particle filters for online nonlinear, non-Gaussian Bayesian tracking. *IEEE Transactions on Signal Processing* **50**, 174–188 (2002).

9. Ionides, E. L., Bretó, C. & King, A. A. Inference for nonlinear dynamical systems. *Proceedings of the National Academy of Sciences of the U.S.A.* **103**, 18438–18443 (2006).

10. Holmgren, J. & Svennerholm, A. M. Mechanisms of disease and immunity in cholera: a review. *Journal of Infectious Diseases* **136**, S105–S112 (1977).

11. Holmgren, J. *et al.* Antitoxic immunity in experimental cholera: Protection, and serum and local antibody responses in rabbits after enteral and parenteral immunization. *Infection and Immunity* **12**, 1331–1340 (1975).

12. Burrows, W., Elliot, M. E. & Havens, I. Studies on immunity to Asiatic cholera. IV. The excretion of copro-antibody in experimental enteric cholera in the guinea pig. *Journal of Infectious Diseases* **81**, 261–281 (1947).

13. Welliver, R. C. & Ogra, P. L. Importance of local immunity in enteric infection. *Journal of the American Veterinary Medical Association* **173**, 560–564 (1978).

14. Svennerholm, A.-M. The Nature of Protective Immunity in Cholera. In *Cholera and Related Diarrheas: Molecular Aspects of a Global Health Problem* (eds. Ouchterlony, Ö. & Holmgren, J.), 195–203 (S. Karger, Basel, 1980).

15. Freter, R. Gut-associated immunity to cholera. In *Cholera* (eds. Barua, D. & Burrows, W.), 315–331 (W. B. Saunders, Philadelphia, 1974).

16. Holmgren, J., Czerkinsky, C., Lycke, N. & Svennerholm, A. M. Mucosal immunity: implications for vaccine development. *Immunobiology* **184**, 157–179 (1992).

17. Pierce, N. F. & Koster, F. T. Stimulation of Intestinal Immunity. In *Acute enteric infections in children: new prospects for treatment and prevention* (eds. Holme, T., Holmgren, J., Merson, M. H. & Mollby, R.), 413–423 (Elsevier/North-Holland Biomedical Press, Amsterdam, 1981).

18. Levine, M. M., Kaper, J. B., Black, R. E. & Clements, M. L. New knowledge on pathogenesis of bacterial enteric infections as applied to vaccine development. *Microbiological reviews.* **47**, 510–550 (1983).

19. Holmgren, J., Andersson, A., Wallerstrom, G. & Ouchterlony, O. Experimental studies on cholera immunization. II. Evidence for protective antitoxic immunity mediated by serum antibodies as well as local antibodies. *Infection and Immunity* **5**, 662–667 (1972).

20. Holmgren, J. & Bergquist, C. Oral B Subunit-Killed Whole-Cell Cholera Vaccine. In *New Generation Vaccines* (eds. Levine, M. M., Kaper, J. B., Rappuoli, R., Liu, M. A. & Good, M. F.), chap. 43, 499–509 (Marcel Dekker, New York, 2004), 3rd edn.

21. Svennerholm, A. M., Holmgren, J., Sack, D. A. & Bardhan, P. K. Intestinal antibody responses after immunisation with cholera B subunit. *The Lancet* **319**, 305–308 (1982).

22. McCormack, W. M., Chakraborty, J., Rahman, A. S. & Mosley, W. H. Vibriocidal antibody in clinical cholera. *Journal of Infectious Diseases* **120**, 192–201 (1969).

23. d'Herelle, F., Malone, R. H. & N., L. M. Studies on Asiatic Cholera. *Indian Medical Research Memoirs* **11**, 1–161 (1930).

24. Monsur, K. A. & Marchuk, L. M. Therapeutic and prophylactic value of cholera phage. In *Cholera* (eds. Barua, D. & Burrows, W.), 273–280 (W. B. Saunders, Philadelphia, 1974).

25. Pollitzer, R. R. Cholera studies. 5. Bacteriophage investigations. *Bulletin of the World Health Organization* **13**, 1–25 (1955).

26. World Health Organization. Cholera vaccines. *Weekly Epidemiological Record* **76**, 117–124 (2001). URL `http://www.who.int/wer`.

27. Kaper, J. B., Morris, J. G. & Levine, M. M. Cholera. *Clinical Microbiology Reviews* **8**, 48–86 (1995).

28. Cash, R. A. *et al.* Response of man to infection with *Vibrio cholerae*. I. Clinical, serologic, and bacteriologic responses to a known inoculum. *Journal of Infectious Diseases* **129**, 45–52 (1974).

29. Levine, M. M. *et al.* Volunteer studies in development of vaccines against cholera and enterotoxigenic *Escherichia coli*: a review. In *Acute enteric infections in children: new prospects for treatment and prevention* (eds. Holme, T., Holmgren, J., Merson, M. H. & Mollby, R.), 443–459 (Elsevier/North-Holland Biomedical Press, Amsterdam, 1981).

30. Glass, R. I. & Black, R. E. The Epidemiology of Cholera. In *Cholera*, 129–154 (Plenum Medical Book Co., New York, 1992).

31. Svennerholm, A. M., Lange, S. & Holmgren, J. Intestinal immune response to cholera toxin: dependence on route and dosage of antigen for priming and boosting. *Infection and Immunity* **30**, 337–341 (1980).

32. Cash, R. A., Music, S. I., Libonati, J. P., Schwartz, A. R. & Hornick, R. B. Live oral cholera vaccine: evaluation of the clinical effectiveness of two strains in humans. *Infection and Immunity* **10**, 762–764 (1974).

33. Merrell, D. S. *et al.* Host-induced epidemic spread of the cholera bacterium. *Nature* **417**, 642–645 (2002).

34. Koelle, K. & Pascual, M. Disentangling extrinsic from intrinsic factors in disease dynamics: a nonlinear time series approach with an application to cholera. *American Naturalist* **163**, 901–913 (2004).

35. Koelle, K., Rodo, X., Pascual, M., Yunus, M. & Mostafa, G. Refractory periods and climate forcing in cholera dynamics. *Nature* **436**, 696–700 (2005).

36. Bjørnstad, O. N., Finkenstädt, B. F. & Grenfell, B. T. Dynamics of measles epidemics: Estimating scaling of transmission rates using a Time series SIR model. *Ecological Monographs* **72**, 169–184 (2002).

37. Grenfell, B. T., Bjørnstad, O. N. & Finkenstadt, B. F. Dynamics of measles epidemics: Scaling noise, determinism, and predictability with the TSIR model. *Ecological Monographs* **72**, 185–202 (2002).

38. Glass, K., Xia, Y. & Grenfell, B. T. Interpreting time-series analyses for continuous-time biological models-measles as a case study. *Journal of Theoretical Biology* **223**, 19–25 (2003).

39. Siddique, A. K. *et al.* Survival of classic cholera in Bangladesh. *The Lancet* **337**, 1125–1127 (1991).

40. Rodo, X., Pascual, M., Fuchs, G. & Faruque, A. S. G. ENSO and cholera: A nonstationary link related to climate change? *Proceedings of the National Academy of Sciences of the U.S.A.* **99**, 12901–12906 (2002).